J Appl Electrochem (2009) 39:1105–1110
DOI 10.1007/s10800-008-9765-2

ORIGINAL PAPER

Improved thermal stability of graphite electrodes in lithium-ion batteries using 4-isopropyl phenyl diphenyl phosphate as an additive

Qingsong Wang · Jinhua Sun · Chunhua Chen

Received: 25 July 2008 / Accepted: 18 December 2008 / Published online: 4 January 2009

Abstract To enhance the thermal stability of graphite electrodes for lithium-ion batteries, 4-isopropyl phenyl diphenyl phosphate (IPPP) was investigated as an additive in the electrolyte of 1.0 M $LiPF_6$ in ethylene carbonate and diethyl carbonate (1:1 in weight). The electrochemical performance of Li/IPPP-electrolyte/C half cells was evaluated. The thermal behavior of Li_xC_6 and Li_xC_6-IPPP-electrolytes were examined using a C80 micro-calorimeter. Electrolytes with 5 and 10% IPPP improve the thermal stability of the graphite electrode in the tests. The electrochemical performance of Li/IPPP-electrolyte/C cells is not degraded by the addition of this amount of IPPP to the electrolyte.

Keywords Lithium-ion battery · Graphite · Thermal behavior · C80 micro-calorimeter · 4-Isopropyl phenyl diphenyl phosphate

1 Introduction

Lithium-ion batteries have a very high energy density, which is four times of that of lead-acid batteries and two to three times of that of nickel–cadmium and nickel–metal hydride batteries. They also have the potential to be one of the lowest cost battery systems [1, 2]. Therefore, lithium-ion battery technology has developed rapidly in the past three decades [3–6]. A lithium-ion cell consists of flammable organic electrolyte and electrodes. Under normal or abusive conditions, fire and explosion may be caused. Thus, the high safety of lithium-ion batteries is an essential requirement for their further development, especially for larger size unit [7–10].

Graphite remains the main choice for anode material in rechargeable lithium-ion batteries because of its high capacity, flat voltage and low cost. However, it is very sensitive to the electrolyte, and if this is not judiciously selected, it may hinder reversible lithium intercalation into the graphite and cause unacceptable capacity loss in the first cycle [11]. The solid electrolyte interphase (SEI) formed on the graphite surface has a crucial impact on battery performance and safety [12, 13]. It is reported that the SEI layer may start to decompose at very low temperatures, even below 60 °C [13, 14] and this provides the necessary energy for thermal runaway [11, 13]. Therefore, the safety maybe improved by inhibiting this process or reducing the heat generation of the reaction [15, 16].

A perfect additive should be able to reduce the lithium-ion battery thermal hazard without deleteriously affecting its original electrochemical performance. Many electrolyte additives have been explored, as reviewed by Zhang [17]. According to the additive functionality, they can be divided into six categories: (1) SEI forming improver, (2) cathode protection agent, (3) $LiPF_6$ salt stabilizer, (4) safety protection agent, (5) Li deposition improver, and (6) other agents such as solution enhancer, Al corrosion inhibitor and wetting agent [17]. 4-Isopropyl phenyl diphenyl phosphate (IPPP) is a new flame retardant agent with good compatibility, anti-flammability and thermal stability [18]. Its molecular formula is $C_{21}H_{21}O_4P$ and the chemical structure is shown in Fig. 1.

Q. Wang (✉) · J. Sun
State Key Laboratory of Fire Science, University of Science and Technology of China, Hefei 230026, Anhui, People's Republic of China
e-mail: pinew@ustc.edu.cn

C. Chen
Department of Materials Science & Engineering, University of Science and Technology of China, Hefei 230026, Anhui, People's Republic of China

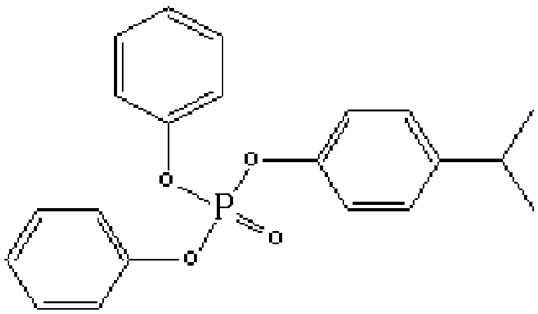

Fig. 1 Chemical structure of IPPP

In our previous study, we reported the use of IPPP as a flame retardant additive for lithium-ion battery electrolytes [18]. The addition of IPPP to the electrolyte reduces its flammability, and delays the onset temperature of the major exothermal reactions. The IPPP effect on the cathode was also studied in enhancing thermal stability [19, 20]. However, the impact of IPPP on graphite anodes in lithium-ion batteries is unclear. Therefore, the effects of IPPP on the thermal stability and electrochemical performance of graphite anodes were studied in this work.

2 Experimental

IPPP (Lianrui Chemical Co.), carbonate solvents (Guotai-Huarong New Chemical Materials Co.) and $LiPF_6$ (Tianjin Jinniu Power Sources Material Co.) were used as received. The solution of 1.0 M $LiPF_6$/ethylene carbonate (EC) + diethyl carbonate (DEC) (1:1 wt%) was prepared in an argon glove box (MBraun Labmaster 130) and used as a standard electrolyte. The graphite electrode used in this study consisted of a mixture of graphite (Hongyuan Carbon Industry Co., Ltd) and polyvinylidene fluoride (PVDF) binder.

The effect of IPPP additive on the cell performance was tested in CR2032 coin cells. The graphite laminate was made of 92% graphite and 8% PVDF binder on copper foil. A Celgard 2400 polyethylene separator (20 μm thick) was used. The graphite laminate was dried 10 h in vacuum at 70 °C and handled in the argon filled glove box (MBraun Labmaster 130, <1 ppm O_2 and H_2O). Then graphite electrodes were punched in disk-shaped pieces of 14 mm diameter and 400 μm thickness. The Li/C cells were assembled with these disks, which provided samples for a C80 experiment. The cells were cycled on a multi-channel battery cycler (Neware BTS-6V10 mA, Shenzhen) at room temperature, between 3.0 V and 0 V at 0.2 mA cm^{-2} current density. Alternating current (AC) impedance measurement was also carried out on the cells with a CHI 604A Electrochemical Workstation. The frequency range and voltage amplitude were set as 10–0.01 Hz and 5 mV, respectively.

The charged cells were then disassembled in an argon filled glove box. To remove the electrolyte from the electrode, the wet charged electrode powder was placed into a bottle. To this bottle a portion of dimethyl carbonate (DMC), a volatile organic solvent, was added and the bottle was then shaken by hand. The sample was then decanted and the DMC rinsing procedure was repeated. After the second decanting, the sample was dried to remove the DMC solvent. As DMC can lead to partial dissolution of the polymeric components of the SEI, which in turn may decrease the integrity and real thermal stability of the SEI, the DMC rinsing procedure was repeated not more than twice. After drying, the electrode material was scraped from the current collectors carefully for thermal testing.

To characterize the thermal stability of the electrodes in the presence of electrolyte, approximately equal amounts of electrode material (including PVDF) and 1.0 M $LiPF_6$/EC + DEC electrolyte were transferred into a high-pressure stainless steel vessel (8.5 ml in volume) of a microcalorimeter (Setaram C80) sealed in argon atmosphere. The weight of each sample (vessel + sample) was measured before and after the experiment to verify that the system was hermetically sealed. The weight was constant in all cases, indicating that there were no leaks during the experiments. The measurements were carried out using a heating rate set at 0.2 °C min^{-1} in the temperature range 30–300 °C in an argon filled vessel. The thermal effects of sample with temperature were thus recorded automatically, and the C80 calculations were based on dry film weight of the electrode material.

3 Results and discussion

3.1 Electrochemical performance of Li/IPPP-electrolyte/C cells

Figure 2 shows the first discharge/charge plots of Li/IPPP-electrolyte/C cells. The cells were cycled between 3.0 V and 0 V at a 0.2 mA cm^{-2} discharge/charge current density. The specific capacity losses in the first cycle for the of Li/C cells with 5, 10, and 15% IPPP content in the electrolyte are 41.1 mAh g^{-1}, 39.2 mAh g^{-1} and 39.7 mAh g^{-1}, respectively, which are little different from them of Li/C cells without IPPP in the electrolyte (43.0 mAh g^{-1}). Therefore, the results indicate that IPPP has little influence on the capacity losses for the first cycle of Li/IPPP-electrolyte/C cells. When the IPPP content increases to 20% in the electrolyte, the capacity loss reaches 50.3 mAh g^{-1}, and the increased capacity loss indicates that more lithium is consumed and the reversible capacity is decreased.

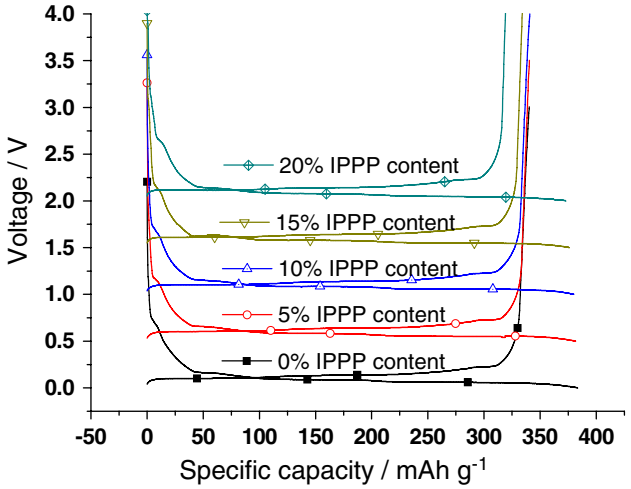

Fig. 2 First discharge/charge plots of Li/C cells with different IPPP content in 1.0 M $LiPF_6$/EC + DEC (1:1 wt%) electrolyte. The cells were cycled between 3.0 V and 0 V at a 0.2 mA cm^{-2} discharge/charge current density (the lines were moved upwards 0.5 in turn for clear)

Hence, IPPP has little influence on the first cycle performance of graphite anode assembled cells, and 5–15% IPPP content in electrolyte is an acceptable concentration judged by this point.

In order to reveal the IPPP effect on cycle efficiency of Li/IPPP-electrolyte/C cells, the cells were cycled between 3.0 V and 0 V at a 0.2 mA cm^{-2} discharge/charge current density, and the results are shown in Fig. 3. Without IPPP in the electrolyte, the cycling efficiency of a Li/C cell is 99.7% in average level, and the standard deviation is 0.83. When IPPP is added to the electrolyte, the average cycling efficiencies of the cells are 98.0, 99.5, 99.7, and 105.3% corresponding to 5, 10, 15, and 20% IPPP content in the electrolyte, respectively, and the standard deviations of the cycling efficiencies increase to 2.07, 4.18, 4.01 and 9.43, respectively. Thus, increase in cycle number, causes the cycling efficiency to fluctuate more and its standard deviation increases with increasing IPPP content. The cycling efficiency of Li/20% IPPP-electrolyte/C cell increases significantly after the 32nd cycle, which may be caused by inhibition of the growth of the SEI film. Efficiency over 100% may be attributed to breakdown of the newly formed film on the graphite, and then the intercalated lithium to moving out and accounting for more capacity. The IPPP content electrolytes with 5, 10, and 15% show little influence on the Li/C cell cycling performance and thus, IPPP content below 15% in electrolyte is acceptable.

Figure 4 shows the discharge capacity plots of Li/IPPP-electrolyte/C cells. The cells were cycled between 3.0 V and 0 V at a 0.2 mA cm^{-2} discharge/charge current density. Without the presence of IPPP in the electrolyte, the discharge specific capacity of Li/C cell decreases with increase in cycle number, and the average specific capacity is 326.0 mAh g^{-1} with 12.2 standard deviation for the first 43rd cycles. The specific capacity of the Li/C cell increases with addition of 5 and 10% IPPP. For the Li/C cells with 5 and 10% IPPP content electrolyte, the average specific capacities are 331.6 and 328.7 mAh g^{-1}, with standard deviation of 14.6 and 26.0, respectively. The increased standard deviations may be caused by the formation of new products on the anode surface by the reactions of IPPP with lithium or electrolyte. The newly formed film blocks the Lithium-ion transfer between the electrolyte and graphite layer. Once the blocked Lithium-ions break out from the film, they result in larger standard deviation of specific

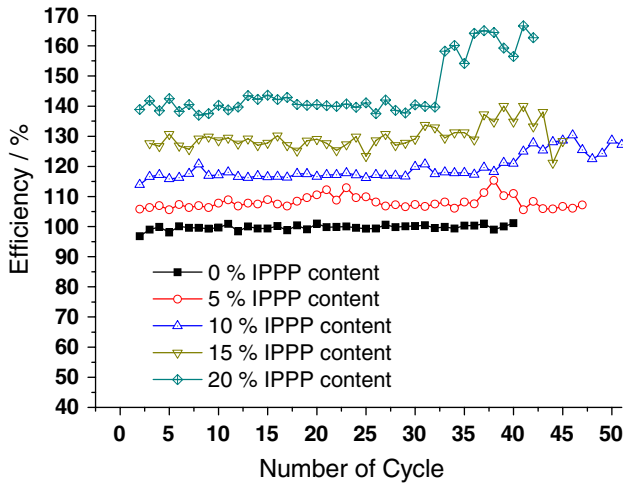

Fig. 3 Cycle efficiencies of Li/C cells with different IPPP content in 1.0 M $LiPF_6$/EC + DEC (1:1 wt%) electrolyte. The cells were cycled between 3.0 V and 0 V at a 0.2 mA cm^{-2} discharge/charge current density (the lines were moved upwards 10 in turn for clear)

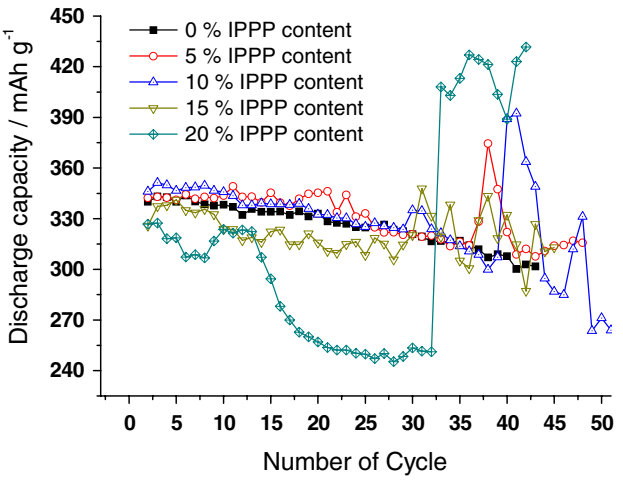

Fig. 4 Discharge capacities of Li/C cells with different IPPP content in 1.0 M $LiPF_6$/EC + DEC (1:1 wt%) electrolyte. The cells were cycled between 3.0 V and 0 V at a 0.2 mA cm^{-2} discharge/charge current density

capacity. The specific capacity decreases to 321.4 mAh g^{-1} when 15% IPPP is added to the electrolyte. Its standard deviation (12.3) is very close to that of Li/C cells without IPPP. After the 30th cycle, its specific capacity fluctuates significantly with the standard deviation of 16.7. When the IPPP content reaches 20%, the specific capacity of the Li/C cell fluctuates significantly in the first several cycles. After the 14th cycle, the capacity drops rapidly. At the 32nd cycle, the capacity drops to 251.2 mAh g^{-1}. The decreased capacity may be due to the blocking of Lithium-ion transfer between electrode and electrolyte by the newly formed film. After the 32nd cycle, the specific capacity is larger than the theoretical capacity (372 mAh g^{-1}). This was also shown in Fig. 3. This phenomenon may be caused by the bursting out of a large amount of embedded lithium-ions in the graphite layers after the blocking SEI film is broken down. From the above results it is speculated that the SEI film formed together with IPPP inhibits the transfer of Lithium-ions between the graphite electrode and electrolyte. When the amount of intercalated lithium reaches a certain level, the film is broken down and the embedded lithium bursts out from the graphite layer very easily, causing the large capacity increase as shown in Fig. 4.

Figure 5 shows the AC impedance test results of Li/C cells with different IPPP content in 1.0 M $LiPF_6$/EC + DEC (1:1 wt%) electrolyte. The cells were cycled three times between 3.0 V and 0 V and then discharged to approximately 0 V. The high frequency semicircle is attributed to the lithium transport through the SEI film of the graphite electrode [21, 22]. Only one semicircle exception for the Li/10% IPPP-electrolyte/C cell was detected, which indicates that a stable SEI film is formed on the graphite surface.

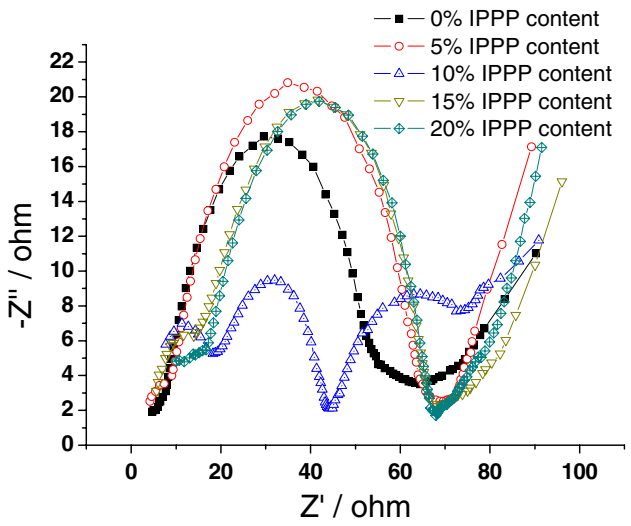

Fig. 5 AC impedances of Li/C cells with different IPPP content in 1.0 M $LiPF_6$/EC + DEC (1:1 wt%) electrolyte. The cells were cycled there cycles between 3.0 V and 0 V and then were discharged approximately to 0 V

The AC impedance of the SEI film is stable and changes very little with the increase in IPPP content in the electrolyte. The AC impedance decreases a little when the IPPP content is 10% in the electrolyte, possibly because 10% IPPP is close to the reactants equivalent ratio. Therefore, the cell assembled using 10% IPPP-added electrolyte has the lowest AC impedance. The SEI film on the anode surface consists of Li_3PO_4 and the oxidation products of IPPP at the discharged states [18, 23]. Therefore, after the addition of IPPP, the SEI film is more stable with less AC impedance increase.

In summary, when the IPPP content in the electrolyte is over 15%, the SEI film formed on the anode is difficult for lithium-ion to pass through, and the specific capacity fluctuates greatly, but with little specific capacity losses. The specific capacity of Li/IPPP-electrolyte/C cells increases when the IPPP content is below 10% because the newly formed SEI film is more permeable at this IPPP content range. Therefore, the addition of 5 and 10% IPPP to the electrolyte does not worsen the electrochemical performance of Li/C cells.

3.2 Thermal stability of lithiated graphite

The anode plays a key role for the thermal runaway of lithium-ion battery, as the SEI formed on the anode surface decomposes at low temperature. The IPPP influence on the Li_xC_6 thermal stability is shown in Fig. 6. The Li_xC_6 were obtained from corresponding Li/IPPP-electrolyte/C cells at approximately 0 V. The single $Li_{0.84}C_6$ obtained from a Li/C cell without IPPP in the electrolyte decomposes at 47 °C. As for the lithiated graphite obtained from Li/5% IPPP-electrolyte/C cells, its SEI film decomposes at 79 °C. The more IPPP is added into the electrolyte, the higher onset temperature of the exothermic reaction between Li_xC_6 and electrolyte is detected. At 10, 15, and 20% IPPP the

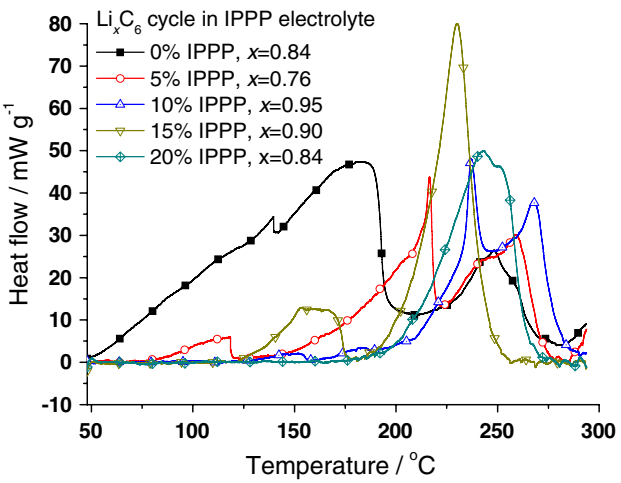

Fig. 6 Heat flows of Li_xC_6 alone at a 0.2 °C min^{-1} heating rate, the Li_xC_6 are got from Li/IPPP-electrolyte/C cells at about 0 V

onset temperatures are 130, 123, and 181 °C, respectively. The results indicate that IPPP restrains the decomposition of Li_xC_6 effectively, and the heat generation decreases greatly. The heat generation was calculated based on the C80 data [24–26]. It was found that, the heat generation is reduced from −491 J g^{-1} (0% IPPP) to −43.4 J g^{-1} (5% IPPP), −13.1 J g^{-1} (10% IPPP), −126.7 J g^{-1} (15% IPPP) and −8.2 J g^{-1} (20% IPPP), and the total heat generation is reduced from −1,339.0 J g^{-1}(0% IPPP) to −715.9 J g^{-1} (5% IPPP), −596.3 J g^{-1}(10% IPPP), −713.6 J g^{-1} (15% IPPP) and −587.8 J g^{-1}(20% IPPP), respectively. Therefore, IPPP improves the thermal stability of Li_xC_6 anodes significantly.

In the actual lithium-ion battery system, the electrolyte coexists with anode, and therefore, the thermal stability of such coexisting system is closely related to the safety of lithium-ion batteries. Figure 7 shows the heat flow plots of Li_xC_6-IPPP-electrolyte at a 0.2 °C min^{-1} heating rate. The Li_xC_6 was obtained from Li/IPPP-electrolyte/C cells at approximately 0 V, and the IPPP content in the electrolyte correspond to that of Li/IPPP-electrolyte/C cells. Three to four exothermic peaks were detected, which are attributable to SEI breakdown, lithium-electrolyte reaction, new SEI film breakdown and Li_2CO_3 formation reactions overlapped with PVDF reactions, respectively [13]. The Li_xC_6 and electrolyte system starts to release heat at 60 °C by the breakdown of SEI film, and reaches its exothermic peak temperature at 102 °C with a heat generation of −495.5 J g^{-1}. Once the IPPP is added to the electrolyte, the onset temperatures of SEI breakdown in the coexisting system increase to 85, 88, 90, and 89 °C for 5% IPPP, 10% IPPP, 15% IPPP and 20% IPPP-electrolyte, respectively. Furthermore, the heat generation of SEI decomposition is reduced to −46.7, −18.2, −16.6, and −22.6 J g^{-1} for 5, 10, 15, and 20% IPPP-added electrolytes, respectively. The results indicate that 5% IPPP in the coexisting system delays the onset temperature of SEI decomposition by approximately 17 °C, and the heat generation is reduced from −495.5 J g^{-1} to −46.7 J g^{-1}.

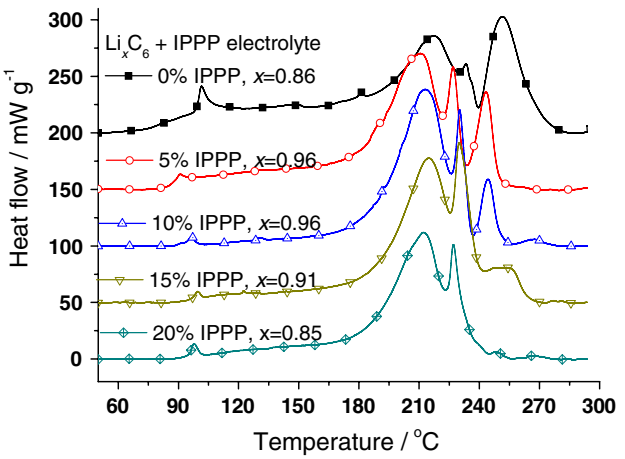

Fig. 7 Heat flows of Li_xC_6-IPPP-electrolyte at a 0.2 °C min^{-1} heating rate, the Li_xC_6 are got from Li/IPPP-electrolyte/C cells at about 0 V, and the IPPP content in electrolyte are corresponding to that of Li/IPPP-electrolyte/C cells (the lines were moved upwards 50 in turn for clear)

It is concluded that, by the addition of IPPP to the electrolyte, the onset temperature of SEI decomposition is significantly delayed and the total heat generation is significantly reduced. The using of IPPP reduces the possibility of the following exothermic reactions and thus the thermal stability of the whole lithium-ion battery system is improved.

4 Conclusions

The effects of the addition of IPPP to the electrolyte on the electrochemical and thermal stability performance of graphite anodes were studied. The electrochemical tests show that when less than 10% IPPP is added to the electrolyte, the electrochemical performance of graphite is similar to the case when no IPPP is added. When the IPPP content is more than 15%, the newly formed SEI film is too robust for lithium-ions to transfer between the electrodes and electrolyte, causing large fluctuations in cycle specific capacity. The thermal stability test results show that IPPP improves the thermal stability of lithiated graphite anodes effectively. The addition of 5% IPPP inhibits the decomposition of SEI films significantly. Based on electrochemical performance and thermal stability studies, it is concluded that the addition of 5 and 10% IPPP to the electrolyte has almost no impact on the electrochemical performance of graphite anodes, but improves its thermal stability significantly; thus, it is an excellent choice of electrolyte additive.

Acknowledgments This study was supported by the National Science Foundation of China (grant no. 20603034) and youth funds of USTC.

References

1. Nagasubramanian G, Ingersoll D, Doughty D, Radzykewycz D, Hill C, Marsh C (1999) J Power Sources 80:116
2. Wakihara M (2001) Mater Sci Eng R 33:109
3. Jansen AN, Kahaian AJ, Kepler KD, Nelson PA, Amine K, Dees DW, Vissers DR, Thackeray MM (1999) J Power Sources 82:902
4. Aurbach D, Gofer Y, Lu Z, Schechter A, Chusid O, Gizbar H, Cohen Y, Ashkenazi V, Moshkovich M, Turgeman R, Levi E (2001) J Power Sources 97–98:28
5. Morford RV, Welna DT, Kellam CE, Hoftnann MA, Allcock HR (2006) Solid State Ionics 177:721
6. Ritchie A, Howard W (2006) J Power Sources 162:809
7. Ritchie AG (2004) J Power Sources 136:285
8. Doughty DH, Roth EP, Crafts CC, Nagasubramanian G, Henriksen G, Amine K (2005) J Power Sources 146:116

9. Wang QS, Sun JH, Yao XL, Chen CH (2006) J Loss Prev Proc 19:561
10. Wang QS, Sun JH, Yao XL, Chen CH (2006) J Solut Chem 35:179
11. Watanabe I, Yamaki J (2006) J Power Sources 153:402
12. Andersson AM, Edstrom K, Rao N, Wendsjo A (1999) J Power Sources 82:286
13. Wang QS, Sun JH, Yao XL, Chen CH (2006) J Electrochem Soc 153:A329
14. Wang QS, Sun JH, Yao XL, Chen CH (2005) Thermochim Acta 437:12
15. Herstedt M, Stjerndahl M, Gustafsson T, Edstrom K (2003) Electrochem Commun 5:467
16. Herstedt M, Rensmo H, Siegbahn H, Edstrom K (2004) Electrochim Acta 49:2351
17. Zhang SS (2006) J Power Sources 162:1379
18. Wang QS, Sun JH, Yao XL, Chen CH (2005) Electrochem Solid State 8:A467
19. Wang QS, Sun JH, Chen CH (2006) J Power Sources 162:1363
20. Wang QS, Sun JH (2007) Mater Lett 61:3338
21. Katayama N, Kawamura T, Baba Y, Yamaki J (2002) J Power Sources 109:321
22. Zhang SS, Xu K, Jow TR (2003) J Power Sources 113:166
23. Yao XL, Xie S, Chen CH, Wang QS, Sun JH, Li YL, Lu SX (2005) J Power Sources 144:170
24. Sun JH, Li YF, Hasegawa K (2001) J Loss Prev Proc 14:331
25. Sun JH, Li XR, Hasegawa K, Liao GX (2004) J Therm Anal Calorim 76:883
26. Wang QS, Sun JH, Lu SX, Yao XL, Chen CH (2006) Solid State Ionics 177:137